Available online at www.sciencedirect.com
SCIENCE DIRECT
Polymer 47 (2006) 3856–3865
polymer
www.elsevier.com/locate/polymer

Dielectric analyses of a series of poly(2-hydroxyethyl methacrylate-*co*-2,3-dihydroxypropyl methacylate) copolymers

K. Mohomed [a], F. Moussy [b], J.P. Harmon [a,*]

[a] *Department of Chemistry, University of South Florida, 4202 East Fowler Avenue, CHE 205, Tampa, FL 33620-5250, USA*
[b] *Department of Chemical Engineering, University of South Florida, 4202 East Fowler Avenue, ENB 118, Tampa, FL 33620-5250, USA*

Received 6 February 2006; received in revised form 20 March 2006; accepted 22 March 2006

Abstract

The dielectric spectra of a series of copolymers of 2-hydroxyethyl methacrylate (HEMA) and 2,3-dihydroxypropyl methacrylate (DHPMA) were investigated. Recently, the full range dielectric spectrum of poly(2-hydroxyethyl methacrylate) was reported. This study looks at the effects on the dielectric behavior as a result of 2,3-dihydroxypropyl methacrylate addition. The dielectric permittivity, ε', and the loss factor, ε'', were measured using a dielectric analyzer in the frequency range of 0.6 Hz to 100 kHz and between the temperature range of −150 and 275 °C. The electric modulus formalism was used to reveal the viscoelastic and conductivity relaxations present in the polymers. Several notable changes were observed as 2,3-dihydroxypropyl methacrylate concentration increased. It was observed through DSC and DEA that the glass transition temperature decreased as DHPMA content increased. The secondary dielectric relaxations were also affected as it was recorded that the activation energy for the γ transition increased and the β relaxation decreased with DHPMA content. Ionic conductivity data prove that DHPMA facilitates ionic mobility more efficiently than HEMA.

Keywords: 2-Hydroxyethyl methacrylate (HEMA); 2,3-Dihydroxypropyl methacrylate (DHPMA); Dielectric relaxation

1. Introduction

We recently reported the full range dielectric response of neat poly(2-hydroxyethyl methacrylate) (PHEMA) from −150 to 275 °C [1]. The dielectric response of dry and hydrated PHEMA had been studied earlier but data obtained above 50 °C had not been reported [2–8]. It was important to decipher the dielectric spectrum of PHEMA to further investigate the effects of a novel hydroxylated nanoparticle on the polymer matrix [9,10]. The electric modulus formalism [11–13] was employed to reveal the various structural and conductivity relaxations present in the polymer composites. The effects of crosslinking and plasticization in the polymer matrices were monitored by characterizing the molecular relaxations present in the polymer and the ionic diffusion in the polymer matrix. Using dielectric spectroscopy, it was determined that the activation energy needed to bring about the molecular relaxation of the pendant groups in composites was highly dependent on the available free volume and that the ionic conductivity activation energy generally increased as the degree of crosslinking increased and it decreased as plasticization effect increased [9,14]. This phenomenon is due to the immobilization (or lack thereof) of the matrix, which consequently hinders (or enhances) the rotational movement of the side chain moiety and the translational diffusion of ions in the matrix [15]. Dielectric analysis proved to be a useful tool to better understand the polymer–filler interface.

In this study, the dielectric spectra of several random copolymers of 2-hydroxyethyl methacrylate (HEMA) and 2,3-dihydroxypropyl methacrylate (DHPMA) are analyzed. The structures of these monomers are shown in Fig. 1. Both of these materials sorb water to form hydrogels, and have found a role in biomedical applications for such materials as contact lenses, bioadhesive gels for drug delivery and as a thrombo- and fibro-resistant coating for implantable sensors [2,16–18]. Gates et al. was the first to report the dielectric response of poly(HEMA–DHPMA) copolymers in 2003 [2]; the hydrogel samples were prepared as powder sandwiched between polyethylene wafers. As a result, the α transition was not resolved, since the glass transition of PHEMA and PDHPMA occurred at a temperature

* Corresponding author. Tel.: +1 813 974 3397; fax: +1 813 974 1733.
E-mail address: harmon@cas.usf.edu (J.P. Harmon).

0032-3861/$ - see front matter © 2006 Published by Elsevier Ltd.
doi:10.1016/j.polymer.2006.03.099

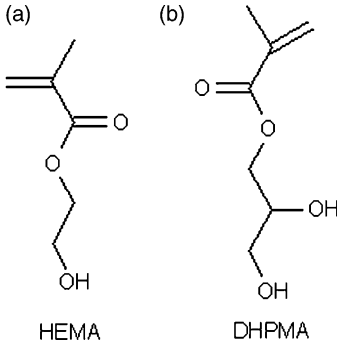

Fig. 1. Chemical structure of (a) 2-hydroxyethyl methacrylate (HEMA) and (b) 2,3-dihydroxypropyl methacrylate (DHPMA).

close to the melt temperature of the polyethylene (Marlex 6000) matrix ($T_m = 120$ °C).

Poly(2,3-dihydroxypropyl methacrylate) (PDHPMA) is also known as glyceryl methacrylate (GMA) and is the major component of Benz-G® materials; the advantage of these materials is that it remains 100% saturated when in contact with the eye [19–21]. The increased water equilibrium content of PDHPMA and its biocompatibility properties have impacted its use as a biomaterial. The recent development of poly(HEMA-*co*-DHPMA) copolymers for use as biocompatible coatings for implantable sensor devices in our laboratory has also prompted this study. Fig. 2 shows a histology image of a pre-hydrated HEMA–DHPMA copolymer subcutaneously implanted in an animal specimen where it is observed that the copolymer induced minimal to no fibrosis. Fig. 3 shows a histology image of the implanted, hydrated, PHEMA homopolymer; as is the case in chronic tissue interaction with the implant, extensive tissue fibrosis occurs and the implanted material becomes encapsulated in scar tissue, which is seen as the dark purple outline at the polymer–tissue interface. The biocompatibility of hydrogels can be attributed to the low interfacial tension with biological fluids, high gas permeability, high diffusion of low molecular weight compounds, and reduced mechanical and frictional irritation to surrounding tissue [22]. This may be due to its increased water equilibrium

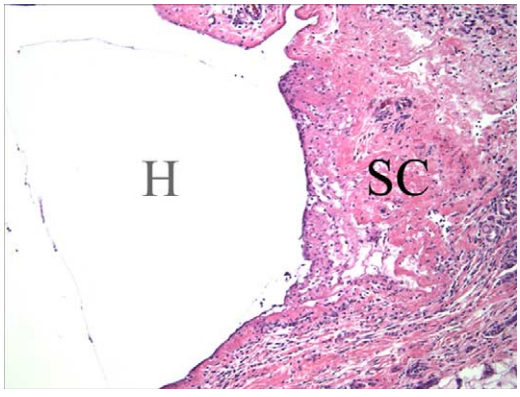

Fig. 2. A histology image of a HEMA–DHPMA copolymer subcutaneously implanted in an animal specimen after 28 days. Hematoxilin and eosin stain. H indicates the location of the hydrogel. SC indicates the subcutaneous tissue.

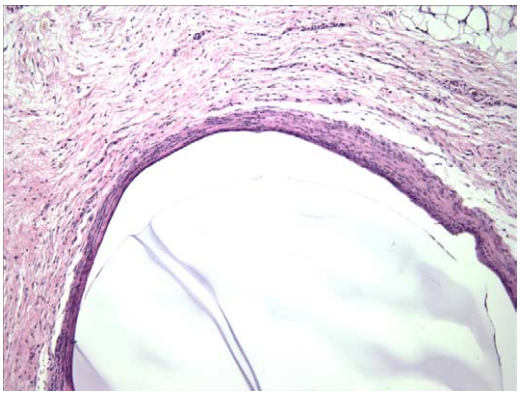

Fig. 3. A histology image of hydrated PHEMA homopolymer subcutaneously implanted in an animal specimen after 28 days showing induced fibrosis at the polymer–tissue interface.

content and porosity of the polymer network. By increasing the DHPMA content in the copolymer, an improvement in biocompatibility was observed; however, the high content DHPMA copolymer and the DHPMA homopolymer were very brittle and fragmented easily when implanted; thereby inducing fibrosis. Further studies are being conducted on the topic of biocompatibility of these copolymers, which will be published in the near future. This present study attempts to fortify previous work to better understand the thermal and dielectric response of these materials up to and above the glass transition region.

Dielectric analysis is an informative technique used to determine the molecular motions and structural relaxations present in polymeric materials possessing permanent dipole moments [11,23]. In dielectric measurements, the material is exposed to an alternating electric field, which is generated by applying a sinusoidal voltage; this process causes alignment of dipoles in the material, which results in polarization. The capacitance and conductance of the material is measured over a range of temperature and frequency, and are related to the dielectric permittivity, ε', and the dielectric loss factor, ε'', respectively. The dielectric permittivity, ε', represent the amount of dipole alignment (both induced and permanent) and the loss factor, ε'', measures the energy required to align dipoles or move ions.

In polymeric materials it has been observed that the loss factor term is a combination of two processes: the rotational reorientation of the permanent dipoles present on the side chains off the polymer backbone, known as a dipolar relaxation and the translational diffusion of ions, which causes conduction and is seen as the conductivity relaxation (Eqs. (1)–(3)) [11,12,23–28].

$$\varepsilon'' = \varepsilon''_{\text{dipole}} + \varepsilon''_{\text{ion}} \tag{1}$$

$$\varepsilon''_{\text{dipole}} = (\varepsilon_R - \varepsilon_U)\frac{\omega\tau_E}{1 + \omega^2\tau_E^2} \tag{2}$$

$$\varepsilon''_{\text{ion}} = \frac{\sigma_{\text{ac}}}{\omega\varepsilon_o} \tag{3}$$

In this paper, various mathematical treatments will be applied to reveal both the viscoelastic and conductivity relaxations present in the dielectric spectra of the poly(HEMA-*co*-DHPMA) copolymers. The authors refer readers to Refs. [1,11] to obtain an in-depth explanation of dielectric theory and its application in characterizing polymers.

2. Experimental

2.1. Materials

2-Hydroxyethyl methacrylate and 2,3-dihydroxypropyl methacrylate monomers were generously donated by Benz R&D (Sarasota, FL). They were used as received without further purification. The free radical initiator employed for the polymerization was Vazo 52® [2,2,′-azobis(2,4-dimethylpentane nitrile)]. Vazo 52®, obtained from Dupont (Wilmington, DE), is a low temperature polymerization initiator that decomposes to form a cyanoalkyl radical.

2.2. Synthesis of poly(HEMA-co-DHPMA) copolymer series

A series of HEMA–DHPMA random copolymers were synthesized using free radical polymerization. 0.2 wt% of the [2,2,′-Azobis(2,4-dimethylpentane nitrile)] Vazo 52® initiator was added to the monomer, which was then degassed with dry nitrogen. The monomers were polymerized for 8 h at 60 °C and then post cured at 115 °C for 4 h. Before thermal and dielectric analysis, the polymer samples were oven dried at 110 °C to constant weight under vacuum and stored under vacuum in the presence of phosphorous pentoxide. The properties of the two homopolymers: PHEMA and PDHPMA, together with three random copolymers of HEMA and DHPMA were investigated.

2.3. Differential scanning calorimetry (DSC)

Experiments were performed on a TA Instruments DSC 2920 to determine the glass transition temperature, T_g, of the polymers. The previously dried sample (4–10 mg) was hermetically sealed in an aluminium pan and a heat–cool–heat cycle was performed. The DSC cell, which was calibrated with indium and kept under an inert nitrogen atmosphere, was heated using a ramp rate of 5 °/min to 140 °C, quench cooled with liquid nitrogen and then reheated at the same rate. The T_g was taken from the second heating cycle.

2.4. Dielectric analysis (DEA)

Single surface dielectric analysis was performed using a TA Instruments DEA 2970. The sample was first chilled with liquid nitrogen and then ground into a fine powder using a Bel Art micromill. The powder was placed on the sensor, heated to 135 °C to embed the sample into the channels of the single surface sensor and then taken down to cryogenic temperatures with liquid nitrogen. A maximum force of 250 N was applied to the sample to achieve a minimum spacing of 0.25 mm. Measurements were taken in 5° increments from −150 to 275 °C through a frequency range of 0.6 Hz to 100 kHz under a dry helium atmospheric purge of 500 ml/min. Capacitance and conductance were measured as a function of temperature and frequency to obtain the dielectric constant, or permittivity (ε'), the dielectric loss (ε'') and the loss tangent ($\tan\delta = \varepsilon''/\varepsilon'$).

Table 1
DSC data: glass transition temperature, T_g, of the HEMA–DHPMA copolymer series

Polymer	Molar ratio HEMA:DHPMA	Actual T_g (°C)	Calculated T_g (°C)
100% HEMA	1:0	101.4	101.4 (act.)
75% HEMA:25% DHPMA	3:1	95.6	96.5
50% HEMA:50% DHPMA	1:1	89.1	92.1
25% HEMA:75% DHPMA	1:3	87.2	88.1
100% DHPMA	0:1	84.4	84.4 (act.)

3. Results and discussion

3.1. Differential scanning calorimetry (DSC)

The glass transition temperatures for the HEMA and DHPMA homopolymers, as well as the random copolymers were determined using differential scanning calorimetry. Differential scanning calorimetry was also used to monitor the drying process, since the presence of water in hydrophilic polymers is known to act as a plasticizer, which will decrease the glass transition temperature, T_g. The drying process was complete when the T_g remained constant even after additional heating under vacuum. The results are listed in Table 1. Prior to polymerization the two monomers were visually miscible and the presence of one glass transition in the copolymers is indicative of this (Fig. 4). The broadening of the transition remained the same for the homopolymers and copolymers at approximately 10 °C. PHEMA and the 50–50 HEMA–DHPMA

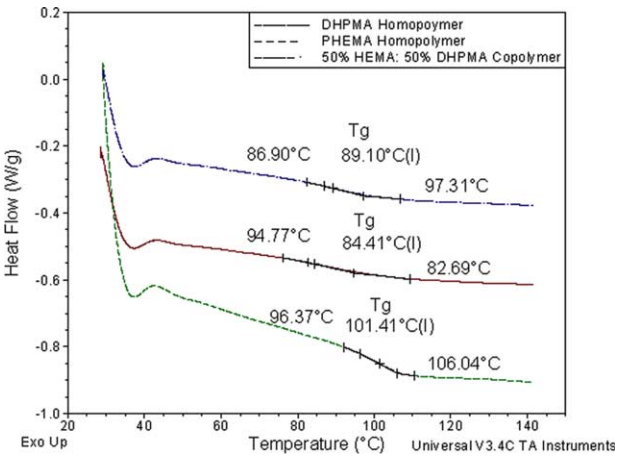

Fig. 4. A plot of the DSC scans for the homopolymers, PHEMA, and PDHPMA, and the 50:50 random copolymer.

copolymer have refractive indices of 1.520 and 1.515, respectively, and both the homopolymers and random copolymers are optically transparent. Unlike previous data reported by Gates et al., the glass transition temperature for this set of copolymers decreased linearly as the DHPMA content increased (with a *R*-squared value of 0.9741). Gates et al. reported a glass transition temperature of 105 °C for both the HEMA and DHPMA homopolymer and the copolymers as well [2]. This difference in reported glass transition temperature may be a result of varying crosslinker content between the samples. The syntheses of the HEMA and DHPMA monomers often result in the production of ethylene glycol dimethacrylate (EGDMA) as an impurity, which acts as a crosslinking agent. The glass transition of the hydrogel will be dependent on the polymerization process, EGDMA concentration and water content present in the polymer. EGDMA is often added to the hydrogel for certain applications where dissolution of the hydrogels needs to be avoided, as in contact lens.

Eq. (4) was used to calculate the theoretical glass transition temperatures of the copolymers based on the experimental T_gs of the homopolymers, where w is the mole fraction of the individual polymer present in the copolymer [29]. Table 1 shows a close semblance between the calculated glass transition temperatures for the copolymers to the actual values.

$$\frac{1}{T_{\text{g copolymer}}} = \frac{w_1}{T_{g1}} + \frac{w_2}{T_{g2}} \tag{4}$$

3.2. Dielectric analysis (DEA)

Mechanical studies show that PHEMA and PDHPMA exhibit two sub-T_g secondary relaxations and a primary glass transition. The transitions are termed α, β, and γ proceeding from the high temperature transition to the low temperature transition. The primary α transition marks the onset of large-scale segmental motion of the main chain, or polymer backbone, and in the case of hydrogels it is affected by factors such as degree of crosslinking and water content. The β relaxation corresponds to the rotation of the ester side group and the γ relaxation is associated with the rotation of the hydroxyl group. Mechanical studies have also shown that the γ relaxation is very pronounced whereas the β relaxation is relatively weak. The β relaxation often appears as a shoulder to the α peak and may even be unresolvable [2,5,8,30]. Dielectric spectroscopy also identifies all three relaxations as the structural groups involved possess dipole moments that interact with the electrical field.

We previously presented an interpretation of the dielectric spectrum of neat PHEMA in which the electric modulus formalism was employed to reveal aspects of the spectrum that is ordinarily hidden as a result of conductivity effects caused by ionic impurities [1]. In this section, a similar approach will be used to characterize the dielectric spectra of PDHPMA and the random copolymers of HEMA and DHPMA.

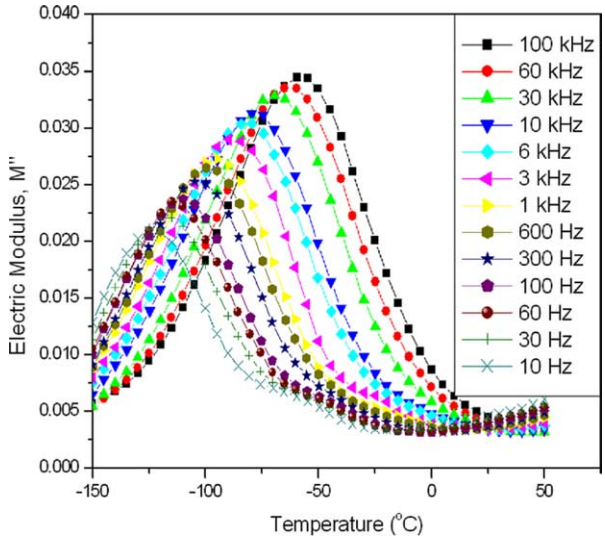

Fig. 5. Electric loss modulus (M'') vs. temperature of the γ relaxation region for PHEMA.

3.2.1. γ Relaxation

It was found that the γ peak was pronounced for the PHEMA, PDHPMA and copolymer samples in both the loss factor and electric loss modulus plots (Figs. 5 and 6). McCrum et al. formulated a mathematical treatment of the complex permittivity, ε^*, which is used to resolve the viscoelastic process from the conductivity effects [11]. By taking the inverse of the complex permittivity, ε^*, one can obtain the electric modulus, M, given by Eq. (5).

$$M^* = \frac{1}{\varepsilon^*} = M' + iM'' = \frac{\varepsilon'}{\varepsilon'^2 + \varepsilon''^2} + i\frac{\varepsilon''}{\varepsilon'^2 + \varepsilon''^2} \tag{5}$$

Plots of the electric loss modulus, M'', vs. temperature show a significant difference from those of ε'' vs. temperature with respect to the separation of the viscoelastic and conductivity relaxations, but technically contain the same information [27]. Due to the placement of the dielectric constant, ε', in the

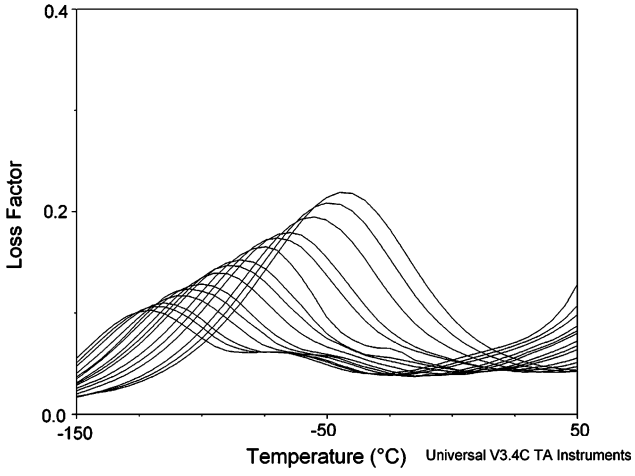

Fig. 6. Loss modulus (E'') vs. temperature of the γ relaxation region for PHEMA.

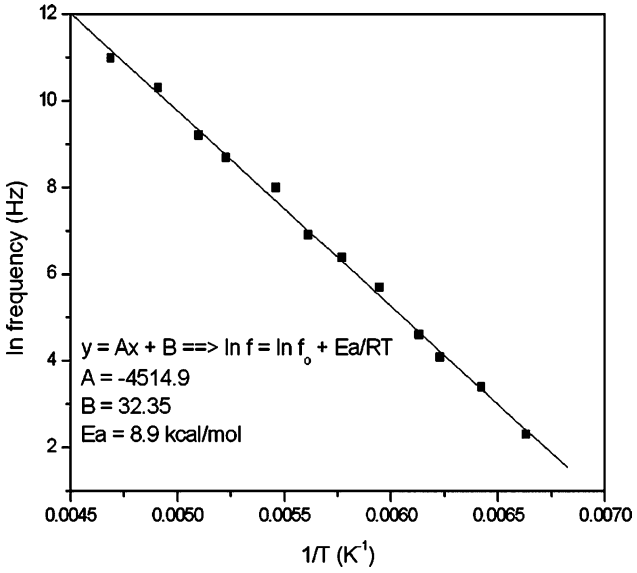

Fig. 7. Arrhenius plot of γ relaxation for PHEMA.

denominator of the equation, its effects in dominating M' and M'' are reduced [26,27]. This allows a more comprehensive analysis of the dielectric data.

The γ relaxation obeyed Arrhenius behavior, which is characteristic of secondary relaxations in polymers. The Arrhenius plot of ln frequency vs. the reciprocal of temperature showed that the peak temperature maxima increased linearly with frequency (Fig. 7) [4,11,29]; the slope of which was used to determine the activation energy from:

$$\ln f = \ln f_o - \frac{\Delta E_a}{RT} \quad (6)$$

The orientation polarization of the –OH side group in PHEMA and PDHPMA is strongly dependent on the dipole moment; the dipole moment of the –OH group is large and is easily aligned in the electric field. The general trend observed was an increase in the activation energy of the γ transition from 8.9 to 15 kcal/mol as the molar concentration of DHPMA increased. It was also observed that the temperature of the peak max increased with DHPMA concentration from −122.3 to −79.8 °C at 10 Hz, as shown in Table 2. As the DHPMA content increased, the γ region also broadened (Fig. 6). This data is in agreement with Gates et al. [2], and is explained by the greater energy needed to overcome the intermolecular interactions brought about by the hydroxyl groups in DHPMA to allow rotation of these groups.

Table 2
DEA data: activation energy and movement of the γ relaxation

Polymer	Activation energy, $E_{A\gamma}$ (kcal/mol)	T_{max} (°C) at 10 Hz	T_{max} (°C) at 100 Hz	T_{max} (°C) at 1000 Hz
PHEMA	8.9	−122.3	−110.0	−94.9
3 HEMA:1 DHPMA	10.3	−109.9	−95.0	−80.7
1 HEMA:1 DHPMA	12.4	−94.9	−79.8	−64.9
1 HEMA:3 DHPMA	13.2	−87.4	−70.0	−55.5
PDHPMA	15.0	−79.8	−64.5	−52.4

3.2.2. α and β Relaxations

The dielectric spectrum of PHEMA showing the occurrence of the β and αβ merge was covered in detail in Ref. [1]. For PHEMA, at low frequencies two M'' peaks were seen, of which one corresponded to the γ relaxation and the other was the β relaxation. The β peak was symmetrical in shape and followed Arrhenius dependency having an activation energy of 24.8 kcal/mol. At frequencies above 6 kHz, a 3rd M'' peak was observed; going from low temperature to high temperature the 1st M'' peak corresponded to the γ relaxation, the 2nd M'' peak represented the αβ merge and the 3rd M'' peak was proven to be the conductivity relaxation. The αβ merge occurred at higher temperatures and frequencies and exhibited non-linear dependency between frequency and temperature [1]. The α relaxation was not completely resolved and in agreement with McCrum et al. and Bergman et al., the β relaxation in methacrylate polymers is faster moving than the α relaxation and tends to merge with the α relaxation [11,25]. The fact that the 3rd M'' peak was a conductivity relaxation based on ionic conduction and not related to any molecular relaxation in the polymer was proven in three ways. Section 3.2.3 briefly shows these proofs but the reader is once again referred to Ref. [1] for a complete explanation.

Fig. 8 shows the full spectra of electric loss modulus, M'', for PHEMA, PDHPMA, and two copolymers; obvious differences can be seen. In neat PHEMA, three M'' peaks were seen, as the DHPMA content increased to 25% (molar), three peaks can still be seen; however, the αβ merge is less resolved at high frequencies. Temperature–frequency plots show that the low frequencies (from 0.6 to 10 Hz) followed a linear Arrhenius relationship, which may be indicative of the β region. However, as frequency increased the relationship deviated from linearity (Fig. 9). This non-linear region is most likely the αβ merge. Fig. 8 shows the β relaxation at multiple frequencies for four out of five copolymers; in which the temperatures at which the β relaxation occurs is seen. The β relaxation as described is the first high temperature symmetrical peak with an Arrhenius relationship, as temperature increases the peak shape, height and temperature dependence changes to indicate the αβ merge (Fig. 9). The temperature at which the β peak occurs shifts toward lower temperatures as DHPMA content increases (Fig. 8).

It should be noted that this is the dielectric beta transition, not the mechanical beta transition. As we have shown in an earlier paper [1], the mechanical peak behaves slightly different from the dielectric peak, where the beta peak is only observable at 1 Hz in the dynamic mechanical analysis (DMA) for the neat PHEMA, the αβ merge was irresolvable at higher frequencies. DMA was not performed for these copolymers, as the polymer became increasingly brittle as the DHPMA content increased.

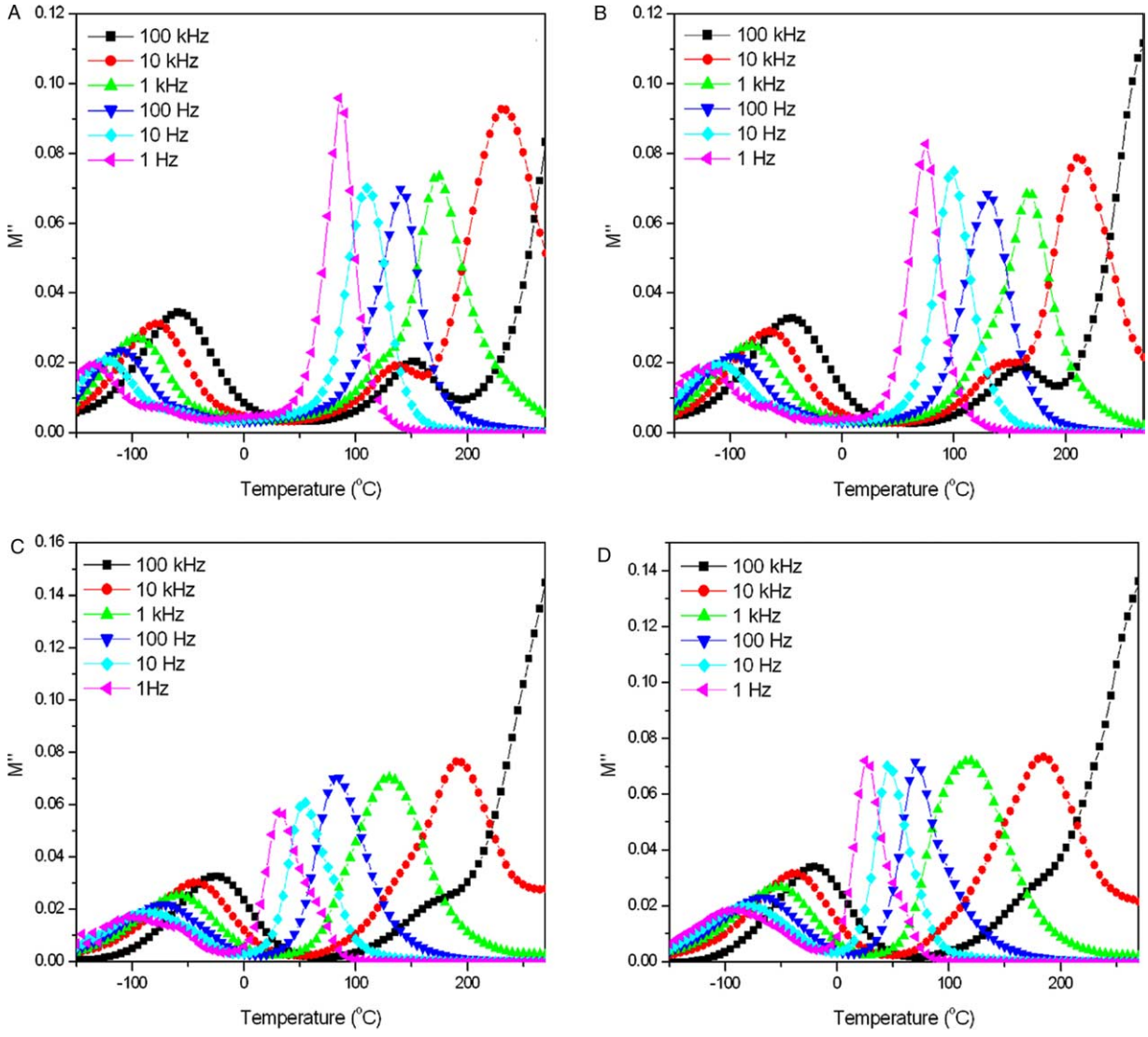

Fig. 8. Electric loss modulus, M'', vs. temperature for (A) PHEMA homopolymer; (B) 75% HEMA:25% DHPMA copolymer; (C) 25% HEMA:75% DHPMA copolymer; and (D) PDHPMA homopolymer.

As the content increased to 50 and 75% DHPMA, one can notice that the 2nd low frequency M'' peak is no longer symmetrical as it was in PHEMA, it has broadened and has a right shoulder (Fig. 8). Conductivity tests (Section 3.2.3) prove that this peak is due to viscoelastic relaxation as it does not fit the conditions for a conductivity peak. Activation energies calculated for the β relaxation using the low frequencies (0.6–10 Hz) follow a trend where the activation energy decreased as DHPMA content increased (Table 3). If the assumption is made that this peak is made up of a cooperative motion between the α and β relaxations drawing from the observation that the peak is not entirely symmetrical as secondary peaks usually are, then this data would support the fact that the glass transition temperature also decreased with DHPMA content as seen in DSC; therefore, less energy would be needed to bring about the transition. Fig. 10 shows the trend observed as DHPMA content increased in the copolymer at 6 kHz.

As DHPMA content increased conductivity effects became more pronounced as it became difficult to resolve the α and β relaxations. The αβ merge in the 50% HEMA:50% DHPMA copolymer became irresolvable as frequency increased; the β relaxation temperature–frequency dependency could only be obtained from low frequencies (0.6–10 Hz). The same was observed as DHPMA content increased. Therefore, only one high temperature viscoelastic relaxation will be depicted for the 50% DHPMA, 75% DMPMA and 100% DHPMA polymers. It is known that the M'' peak at these frequencies are due to viscoelastic relaxation; whereas as the frequency increased the M'' peak exhibited conductivity relaxation characteristics.

3.2.3. Conductivity relaxation

Three different proofs were shown in [1] verifying that the anomalous 2nd M'' high temperature peak observed in the loss modulus plot of PHEMA was in fact not a contribution of

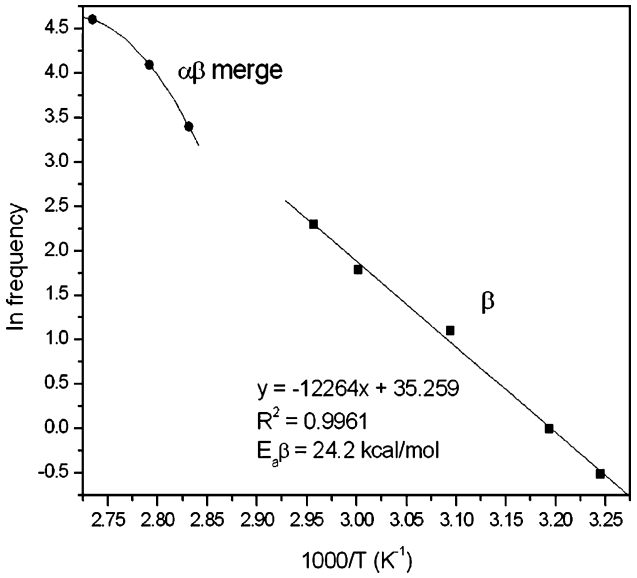

Fig. 9. Temperature–frequency dependency of the β and αβ merge relaxations for the 75% HEMA–25% DHPMA copolymer.

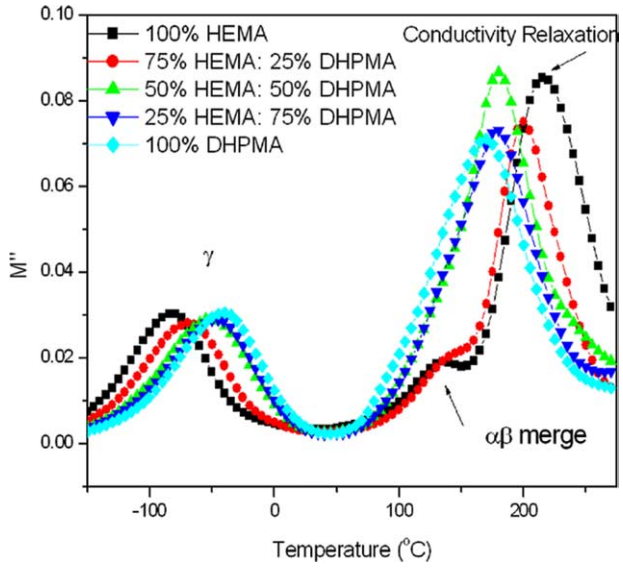

Fig. 10. Comparison of M'' at 6000 Hz for PHEMA, PDHPMA and the copolymers.

viscoelastic relaxation but a result of ionic conduction. The translational diffusion of ions, which causes conduction is seen as a conductivity relaxation and in glass forming polymers this process takes place with increasing viscous flow and usually overpowers the viscoelastic α process in the dielectric loss factor spectra [12,24,25,27].

Proof 1 explains that if the Argand plot, obtained in the region where the 2nd high temperature M'' peak is observed, reveals a true semicircular arc it can be interpreted to mean that it is indeed not a viscoelastic relaxation. Eq. (7) below describes the behavior of a molecule, or rigid polar liquid, having a single relaxation time. Fig. 11 shows the Argand plot of PDHPMA where the values proceed from lower to higher frequencies. The semi-circular arc is characteristic of the Debye model. Both the homopolymers and the series of copolymers exhibited semi-circular Debye plots at temperatures above the glass transition region. Viscoelastic relaxations in polymers, on the other hand, deviate from semicircular behavior in which they exhibit a distribution of relaxation times and are often characterized by modified Cole–Cole expressions [11].

$$\left\{M' - \frac{(M_U + M_R)}{2}\right\}^2 + (M'')^2 = \left(\frac{M_U - M_R}{2}\right)^2 \quad (7)$$

Table 3
DEA data: β relaxation and ionic conductivity activation energy

Polymer	β activation energy (kcal/mol) (0.6–10 Hz)	Ionic conductivity activation energy (kcal/mol)
PHEMA	24.8	10.1
3 HEMA:1 DHPMA	24.2	9.9
1 HEMA:1 DHPMA	21.5	7.1
1 HEMA:3 DHPMA	20.0	6.3
PDHPMA	19.1	5.6

Comparing the Argand plots of the copolymer series two observations were made: (1) the Argand plot generated from the conductivity relaxation region (200 °C) is semi-circular following the Debye model; whereas the plot in the glass transition region (100 °C) deviates from Debye behavior and (2) as DHPMA content increases the Argand plot in the glass transition region appears to look more like a semi-circle. This is another indication that the αβ region in high DHPMA content copolymers is affected by conductivity more than in high HEMA content copolymers.

The second proof involved fitting the data to Eq. (8), an equation derived by Ambrus et al. in which the electric modulus is presented in terms of time, frequency, and modulus

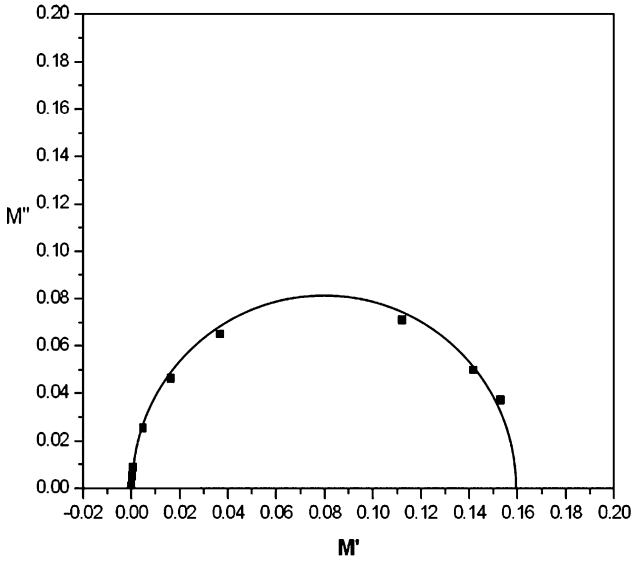

Fig. 11. Argand plot derived from the conductivity relaxation region (200 °C) for poly(2,3-dihydroxypropyl methacrylate).

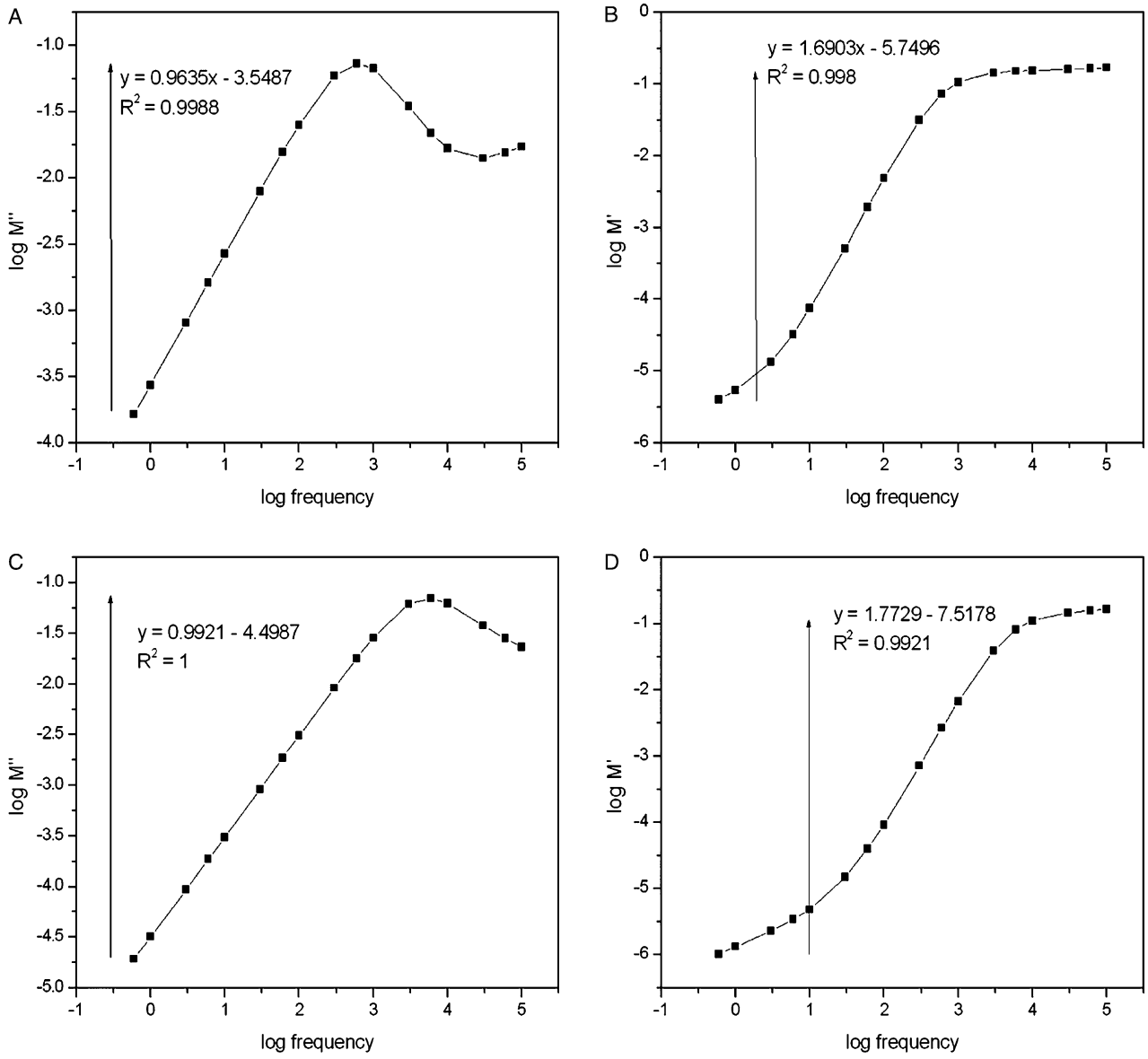

Fig. 12. Dependence of M' and M'' on frequency in the conductivity relaxation region (165 °C) for the homopolymers: poly(2-hydroxyethyl methacrylate) and poly(2,3-dihydroxypropyl methacrylate). (A) M'' dependence for PHEMA; (B) M' dependence for PHEMA; (C) M'' dependence for PDHPMA; (D) M' dependence for PDHPMA.

[13]. Starkweather et al. also employed this equation to show that plots of log M'' and log M' vs. log frequency will reveal slopes of 1 and 2, respectively, if the electric modulus (M) is due purely to ionic conduction as a result of ionic diffusion and independent of viscoelastic, dipolar relaxation [23,27]. Both the homopolymers and the series of copolymers revealed slopes of 1 and 2 for M'', M' dependence on frequency at temperatures above the glass transition region. Fig. 12 shows these plots for neat PHEMA and neat PDHPMA.

$$M = M_s\left(\frac{i\omega\tau_\sigma}{1+\mathrm{i}(\omega\tau_\sigma)}\right) = M_s'\left[\frac{(\omega\tau_\sigma)^2}{1+(\omega\tau_\sigma)^2}\right] + \mathrm{i}M_s''\left[\frac{\omega\tau_\sigma}{1+(\omega\tau_\sigma)^2}\right] \quad (8)$$

It is interesting to note that as the DHPMA content increased the slope value approached the ideal value. For example, the actual slope for the M' plot and the M'' plot for neat PHEMA is a 1.69 (ideal = 2) and 0.96 (ideal = 1); whereas the actual slope for the M' plot and the M'' plot for neat PDHPMA is a 1.77 and 0.99, respectively. This fact establishes the interpretation that conductivity effects are more dominant in DHPMA than HEMA.

When viscoelastic effects are negligible the loss factor is described by Eq. (3). Fig. 13 shows plots of the frequency dependence of ac conductivity (σ_{ac}) for temperatures above T_g where conductivity is predominant for both the homopolymers. Dc conductivity (σ_{dc}) was obtained by extrapolation to zero frequency. As temperature is increased, the frequency dependence of ac conductivity plateaus and is independent of

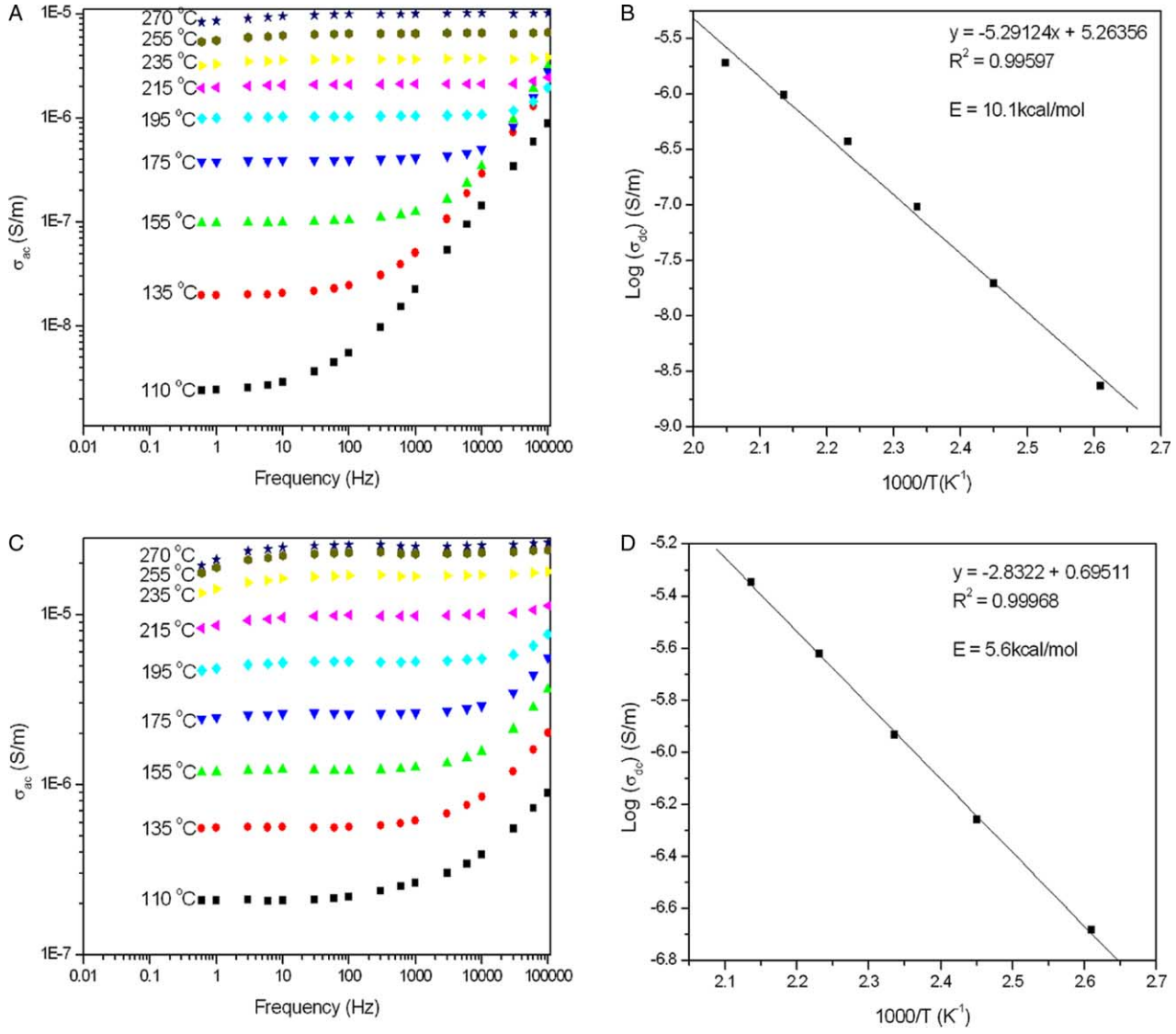

Fig. 13. Frequency dependence of ac conductivity for the homopolymers: poly(2-hydroxyethyl methacrylate) and poly(2,3-dihydroxypropyl methacrylate). (A) Ac conductivity dependence for PHEMA; (B) ionic conductivity activation energy for PHEMA; (C) ac conductivity dependence for PDHPMA; (D) ionic conductivity activation energy for PDHPMA.

all frequencies measured. Dc conductivity (σ_{dc}) follows an Arrhenius relationship expressed by the Eq. (9), where E is the apparent activation energy, k is Boltzmann's constant and σ_o is the pre-exponential factor [31].

$$\log \sigma_{dc} = \log \sigma_o \exp\left(\frac{-E}{kT}\right) \tag{9}$$

Table 3 shows the ionic conductivity activation energy for the copolymers. The ionic conductivity activation energy is the energy required to bring about the translation diffusion of ions in the polymer matrix. As shown in Table 3, the activation energy decreased, from 10.1 to 5.6 kcal/mol, as DHPMA content increased. Therefore, it can be concluded that DHPMA facilitates ionic movement through the polymer matrix better than HEMA; a conclusion also determined by Gates et al. whose ion transport studies showed higher ion diffusion (of both Na^+ and K^+) in PDHPMA than PHEMA [32].

Impurities, such as water and ions, can affect the dielectric data presented, but it is believed that the data is representative of the network structure for the homo- and copolymers presented in this study. A previous study by Gates et al. demonstrated that the diffusivity of a solute through a physically cross-linked membrane increases as the volume fraction of water within the gel increases, and is was observed that the ionic diffusion in hydrated HEMA–DHPMA copolymers increased with increasing DHPMA content [32]. Our research illustrates how dielectric analysis can be used to verify differences in the network structure of the zerogel polymers, where the activation energy for ionic conductivity decreased as DHPMA content increased, this data corroborated with DSC indicate that PDHPMA has a larger matrix than PHEMA.

4. Conclusion

The dielectric spectra of a series of copolymers of 2-hydroxyethyl methacrylate (HEMA) and 2,3-dihydroxypropyl methacrylate (DHPMA) have been investigated. A previous study presented an interpretation of the dielectric spectrum of PHEMA where the electric modulus formalism was used to reveal the viscoelastic and conductivity relaxations present in the polymer. This study looked at the effects on the dielectric behavior as a result of 2,3-dihydroxypropyl methacrylate additions. To the best of the authors' knowledge, this is the first study presenting the dielectric response of these materials up to and above the glass transition region. It was important to study this as DHPMA has been proven to be an excellent material for bio-applications, and is often used as a co-monomer unit with HEMA.

Several notable changes were observed as 2,3-dihydroxypropyl methacrylate concentration increased. The glass transition temperature decreased, the γ activation energy increased, the β activation energy decreased and ionic conductivity increased with DHPMA content. Overall, it was noted as DHPMA content increased conductivity effects became more pronounced as it became difficult to resolve the α and β relaxations, and that DHPMA facilitates ionic movement through its matrix more efficiently than HEMA.

Acknowledgements

This work was supported in part by the National Institute of Health (Grant no. 5R01EB001640-02). We thank Dr F. Moussy and Dr B. Yu for conducting the biocompatibility studies of the hydrogels and for the histology image shown in this paper. The authors would also like to thank Dr J. Ors and Dr P. Benz at Benz Research and Development (Sarasota, FL) for their generous supply of high purity 2-hydroxyethyl methacrylate and 2,3-dihydroxypropyl methacrylate monomers.

References

[1] Mohomed K, Gerasimov TG, Moussy F, Harmon JP. Polymer 2005; 46(11):3847–55.
[2] Gates G, Harmon JP, Ors J, Benz P. Polymer 2003;44(1):207–14.
[3] Diaz Calleja R. J Polym Sci, Part B: Polym Phys 1979;17:1395–401.
[4] Gomez Ribelles JL, Diaz Calleja R. J Polym Sci, Part B: Polym Phys 1985;23:1297–307.
[5] Russell GA, Hiltner PA, Gregonis DE, deVisser AC, Andrade JD. J Polym Sci, Part B: Polym Phys 1980;18:1271–83.
[6] Pathmanathan K, Johari GP. J Polym Sci, Part B: Polym Phys 1990;28: 675–89.
[7] Johari GP. J Mol Struct 1991;250:351–84.
[8] Janacek J. J Macromol Sci, Rev Macromol 1973;9(1):1–47.
[9] Mohomed K, Gerasimov TG, Abourahma H, Zaworotko MJ, Harmon JP. Mater Sci Eng, A 2005;409(1–2):228–34.
[10] Mohomed K, Abourahma H, Zaworotko MJ, Harmon JP. Chem Commun 2005;26:3277–9.
[11] McCrum NG, Read BE, Williams G. Anelastic and dielectric effects in polymeric solids. New York: Dover; 1967.
[12] Macedo PB, Moynihan CT, Bose R. Phys Chem Glasses 1972;13(6): 171–9.
[13] Ambrus JH, Moynihan CT, Macedo PB. J Phys Chem 1972;76(22): 3287–95.
[14] Dahmouche K, Santilli CV, Pulcinelli SH. J Phys Chem B 1999;103: 4937–42.
[15] Eloundou JP, Gerard JF, Pascault JP, Kranbuehl D. Macromol Chem Phys 2002;203:1974–82.
[16] Craig DQM, Tamburic S. Eur J Pharm Biopharm 1997;44:61–70.
[17] LaPorte RJ. Hydrophilic polymer coatings for medical devices. Pennsylvania: Technomic; 1997.
[18] Shtilman MI. Polymeric biomaterials: part 1-polymer implants, new concept in polymer science series. Boston: VSP; 2003.
[19] Benz PH, Ors JA. Contact lens having improved dimensional stability. United States Patent US6011081; 2000.
[20] Benz PH, Ors JA. Contact lens of high water content and high water balance. United States Patent US6096799; 2000.
[21] Benz PH, Ors JA. Terpolymer for contact lens. United States Patent US5891932; 1999.
[22] Kejlova K, Labsky J, Jirova D, Bendova H. Toxicol In Vitro 2005;19: 957–62.
[23] Avakian P, Starkweather Jr. HW, Kampert WG. In: Cheng SZG, editor. Dielectric analysis of polymers. Handbook of thermal analysis and calorimetry, vol. 3. New York: Elsevier; 2002. p. 147–64.
[24] Johari GP, Pathmanathan K. Phys Chem Glasses 1988;29(6):219–24.
[25] Bergman R, Alvarez F, Alegria A, Colmenero J. J Chem Phys 1998; 109(17):7546–55.
[26] Ambrus JH, Moynihan CT, Macedo PB. J Phys Chem 1972;76(22): 3287–95.
[27] Starkweather Jr. HW, Avakian P. J Polym Sci, Part B: Polym Phys 1992; 30:637–41.
[28] Sun Y, Zhang Z, Wong CP. Polymer 2005;46:2297–305.
[29] Gedde UW. Polymer physics. New York: Chapman & Hall; 1995.
[30] Kolarik J. In: Cantow HJ, editor. Secondary relaxations in glassy polymers. Advances in polymer science, vol. 46. New York: Springer; 1982. p. 119–61.
[31] Polizos G, Kyritsis A, Shilov VV, Shevchenko VV. Solid State Ionics 2000;136–137:1139–46.
[32] Gates G, Harmon JP, Ors J, Benz P. Polymer 2003;44(1):214–22.